Thermal Expansion and Magnetostriction of $Ce_{1-x}La_xRhIn_5$

Shawna Hollen
NHMFL

Theory and Introduction

Thermal expansion and magnetostriction are bulk properties of a material that give us information about the inner workings of the lattice and its components. The volumetric thermal expansion of a material is derived from the Maxwell relations and describes the change in volume as a function of temperature at a constant pressure. Likewise, magnetostriction describes volumetric changes as a function of magnetic field at constant temperature and pressure:

$$a_V = \frac{1}{V}\frac{2V}{2T},$$

$$m_V = \frac{1}{V}\frac{2V}{2H},$$

where α_v is the coefficient of volumetric thermal expansion, λ_v is the coefficient of volumetric magnetostriction, V is the volume of the material, T is the temperature, and H is the applied magnetic field. Experimentally, it would be very difficult to measure the volume of a material as you vary the temperature or magnetic field so experimentalists will usually only measure the change in size of one dimension at a time. The coefficients measured from each side can then be added to find the total volumetric thermal expansion or magnetostriction of the material. This may seem to be a cumbersome project, luckily, however, most materials have a regular crystal structure that will simplify the measurement. For example, in a cubic paramagnetic lattice all sides of the unit cell are equal lengths and have antiparallel dipoles. Therefore the thermal expansion and magnetostriction are equal in all directions and,

$a_V = 3a_L$, and

$m_V = 3m_L$.

In a tetragonal structure two sides are equal and a third side is not. Here the expression for thermal expansion is:

$$a_V = 2a_a + a_c,$$

where the axes of the lattice are *a*, *b* and *c* and *a* is the same length as *b*. Furthermore, the general expression for volumetric magnetostriction for any lattice and any magnetism is:

$$m_V = m_a + m_b + m_c.$$

Thermal expansion is closely linked to other thermodynamic properties of a material through the Maxwell relations; therefore by having information about one of these properties, you automatically have information about all of them. An example of this would be the relationship between the heat capacity and the thermal expansion of a material, first observed by Grüneisen. Grüneisen noticed that α_v/C was essentially constant at low temperatures (where C is the heat capacity). He expressed this as:

$$\frac{\alpha_v}{C} = c\,\frac{1}{V},$$

where κ is compressibility, V is volume and γ is a dimensionless proportionality constant known as the Grüneisen parameter.

Dilatometer

To measure thermal expansion accurately it is convenient to use a method of measuring capacitance. By measuring the capacitance between two parallel plates you can find the distance between the plates through a very simple expression:

$$C = \frac{\varepsilon_0 A}{d},$$

where A is the surface area of one of the plates, d is the distance between them, and ε_0 is the permittivity of free space, a well known constant with the value $10^7/4\pi c^2$ or 8.842 x 10^{-11} $(m^2/s^2)^{-1}$. The accuracy of the measurement depends only on how accurately the instrument can measure the capacitance, which means that an apparatus using capacitance to measure thermal expansion can have a very high degree of accuracy. A typical capacitance bridge can measure digits accurately up to 10^{-18} F—eighteen digits after the decimal place (six digits in picoFarads, the unit used on most capacitor bridge displays). Using this information we can calculate, theoretically, how accurately we should be able to measure changes in the size of a sample in a parallel capacitor plate apparatus:

$$C = \frac{\varepsilon_0 A}{d},$$

$$\left|\frac{\partial C}{\partial d}\right| = \frac{\varepsilon_0 A}{d^2},$$

using the fact that $\frac{\partial C}{\partial d} \cdot \frac{\partial C}{\partial d}$, $\Delta d = \Delta C\, d^2/\varepsilon_0 A$, and if you use values so that $d \approx 1cm$ and $A \approx \pi \times 10^{-2}\ m^2$ and the fact that accuracy of the capacitance $\Delta C \approx 10^{-18}$,

$$\partial d \cdot \frac{(10^{-18} F)(10^{-2} m)^2}{(8.842 \# 10^{-11} (m^2/s^2)^{-1})(r\ \# 10^{-2} m^2)} = 3.6 \# 10^{-11} m;$$

which is equivalent to 0.1 *Å*—a tenth of the distance between atoms! Measurements of this resolution can reveal what's happening to a lattice on an atomic level.

In order to achieve this resolution, the dilatometer design and assembly is extremely important. In the experiment that I helped Victor Correa conduct, the cell (Figure 1) consists of two parallel plates each being 1.11 cm in diameter (a. and b.) where the sample is mounted underneath the bottom capacitor plate (b.), allowing the bottom plate to move vertically when the sample expands or contracts. The initial distance between the plates is set by adjusting the screw (d.) to change the height of the sample and the plates that secure it (b., c., and the sample move as a unit). The springs act to secure the sample between the two plates and are mounted around poles for stability and guidance. The advantage of mounting the sample underneath the bottom capacitor plate rather than simply between the plates is mainly so that you can use the definition of capacitance, $C = \frac{f_0 A}{d}$, which is defined with the restriction that the space between the plates is a perfect vacuum (and not a chunk of material). It would also be difficult to mount a metallic material between the plates of a capacitor without shorting the circuit.

One of the things that must be measured before one can make accurate calculations of the distance between the

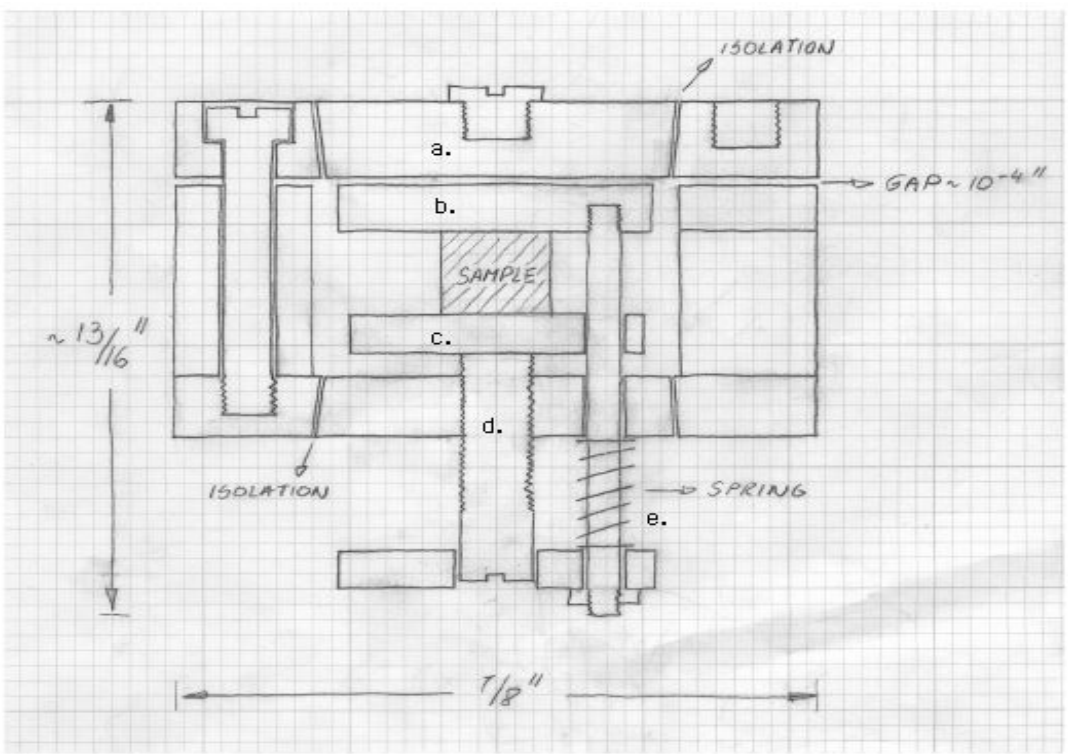

Figure 1:
Dilatometer design.

plates is the constant A—the surface area of a plate. It would be possible to calculate A from the diameter of the capacitor plates, however it is much more accurate to simply measure $\varepsilon_0 A$ with a known distance and capacitance. Measuring the capacitance at a number of different distances and plotting C vs. $1/d$ should produce a straight line with a slope corresponding to your experimental proportionality constant between distance and capacitance. Figure 2 shows the calibration we produced for our dilatometer with an experimental proportionality constant of 8.80 x 10^6 pF•Å. Our theoretical value is 8.6 x 10^6 •Å; which turns out to be very close to our experimental result—a satisfying reassurance.

With this constant we are able to change our measured capacitances to distances and plot them versus the temperature at which they were measured. Since the change in distance between the plates is equivalent to the amount the sample has expanded or contracted, the linear thermal expansion of the sample is the derivative of this curve, $\alpha_L = \frac{-1}{d}\frac{2d}{2T}$. If we then rotate the sample (assuming it has a tetragonal lattice) and measure the linear thermal expansion along one of the other two axes we can easily translate the linear thermal expansion into volumetric thermal expansion:

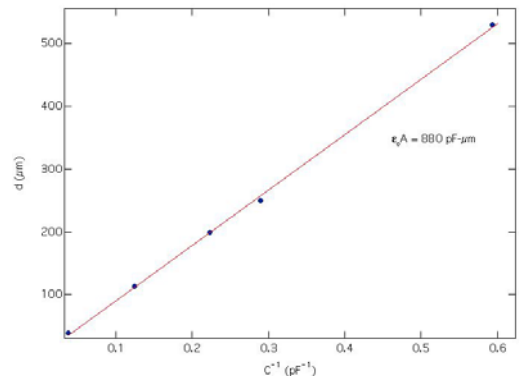

Figure 2: *Calibration*

$$\alpha_V = 2\left(\frac{1}{d_a}\frac{2d_a}{2T}\right) + \frac{1}{d_c}\frac{2d_c}{2T}.$$

Similarly, the magnetostriction of the sample can be calculated as follows:

$$\mu_V = 2\left(\frac{1}{d_a}\frac{2d_a}{2H}\right) + \frac{1}{d_c}\frac{2d_c}{2H}.$$

Cell Effect

One unavoidable problem that can dramatically alter the results of a measurement measurement is the thermal expansion of the cell. Inevitably, the dilatometer will also expand and contract as the temperature of the apparatus changes. The cell effect will change the distance between the capacitor plates regardless of whether or not a sample is mounted. Ideally, it would be nice to 'erase' this effect. One way to attempt this is to measure the thermal expansion of the material that the cell is composed of, and then simply subtract this from the measured thermal expansion of the sample. The cell we used for our measurements is made of oxygen-free high conductivity (OFHC) copper, and to determine the cell effect we mounted a 27mm^3 copper cube and measured the

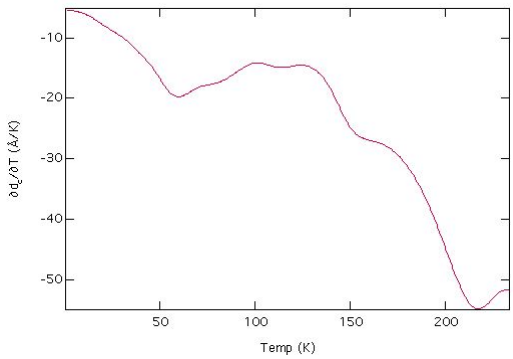

Figure 3: *Cell Effect*

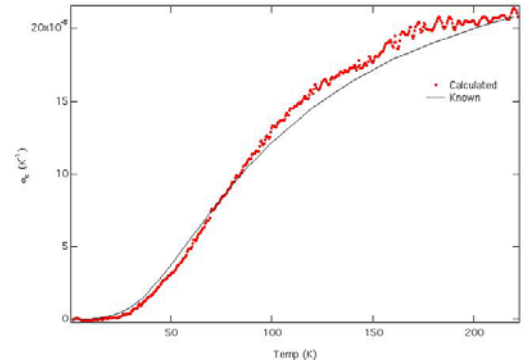

Figure 4: *Aluminum data calculated from cell effect compared to published data.*

thermal expansion several times over a wide range of temperatures. To test the reliability of our cell effect, we measured the thermal expansion of a 27mm^3 aluminum cube and compared our calculated results (taking the cell effect into account) with well-known published results. Figure 3 shows our cell effect and Figure 4 shows that the published results do indeed match our measurements.

We calculated the thermal expansion of aluminum by looking closely at the components of our cell that would affect the distance between the capacitor plates, shown in Figure 5. Following is the derivation of the coefficient of thermal expansion for any sample in our cell. First notice that:

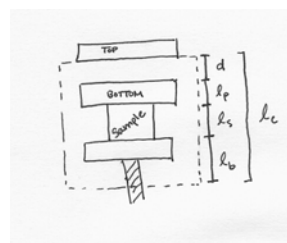

Figure 5: *Components considered for cell effect calculation.*

$$l_c = d_s + l_p + l_s + l_b^s,$$

and if a copper sample is used:

$$l_c = d_{Cu} + l_p + l_{Cu} + l_b^{Cu}.$$

Therefore,

$$l_s = l_c - l_p - d_s - l_b^s,$$

and because the definition of thermal expansion for any sample in the cell is,

$$\alpha_s = \frac{1}{l_s}\left(\frac{2l_s}{2T}\right),$$

we can differentiate the equation for l_s to find α_s:

$$\frac{1}{l_s}\left(\frac{2l_s}{2T}\right) = \frac{1}{l_s}\frac{2}{2T}\left(l_c - l_p - d_s - l_b^s\right).$$

This can be simplified by using

$$l_c - l_p = d_{Cu} + l_{Cu} + l_b^{Cu}$$

from the above equation for l_c in the case of a copper sample in the cell, so that

$$\frac{1}{l_s}\left(\frac{2l_s}{2T}\right)=\frac{1}{l_s}\frac{2}{2T}\left(d_{Cu}+l_{Cu}+l_b^{Cu}-d_s-l_b^s\right).$$

Distributing with foresight produces,

$$\frac{1}{l_s}\left(\frac{2l_{Cu}}{2T}\right)+\frac{1}{l_s}\left(\frac{2(d_{Cu}-d_s)}{2T}\right)+\frac{1}{l_s}\left(\frac{2l_b^{Cu}}{2T}\right)-\frac{1}{l_s}\left(\frac{2l_b^s}{2T}\right),$$

where we will now use the fact that $l_{Cu}/l_{Cu}=l_b^{Cu}/l_b^{Cu}=l_b^s/l_b^s=1$:

$$\frac{l_{Cu}}{l_s}\frac{1}{l_{Cu}}\left(\frac{2l_{Cu}}{2T}\right)+\frac{1}{l_s}\left(\frac{2(d_{Cu}-d_s)}{2T}\right)+\frac{l_b^{Cu}}{l_s}\frac{1}{l_b^{Cu}}\left(\frac{2l_b^{Cu}}{2T}\right)-\frac{l_b^s}{l_s}\frac{1}{l_b^s}\left(\frac{2l_b^s}{2T}\right).$$

Finally, we notice that l_{Cu}, l_b^{Cu}, and l_b^s are all copper and therefore,

$$\frac{1}{l_{Cu}}\left(\frac{2l_{Cu}}{2T}\right)=\frac{1}{l_b^{Cu}}\left(\frac{2l_b^{Cu}}{2T}\right)=\frac{1}{l_b^s}\left(\frac{2l_b^s}{2T}\right)=\alpha_{Cu}.$$

Subsituting we have:

$$\frac{l_{Cu}}{l_s}\alpha_{Cu}+\frac{1}{l_s}\left(\frac{2(d_{Cu}-d_s)}{2T}\right)+\frac{l_b^{Cu}}{l_s}\alpha_{Cu}-\frac{l_b^s}{l_s}\alpha_{Cu}=\left(\frac{l_{Cu}+l_b^{Cu}-l_b^s}{l_s}\right)\alpha_{Cu}+\frac{1}{l_s}\left(\frac{2(d_{Cu}-d_s)}{2T}\right).$$

At room temperatures with samples of comparable sizes,

$l_{Cu}+l_b^{Cu}\ll l_s+l_b^s$, and $l_{Cu}+l_b^{Cu}-l_b^s\ll l_s(RT)$.

Therefore,

$$\left(\frac{l_{Cu}+l_b^{Cu}-l_b^s}{l_s}\right)\ll\frac{l_s(RT)}{l_s(T)}\ll 1,$$

and finally,

$$\alpha_s\ll\alpha_{Cu}+\frac{1}{l_s}\left(\frac{2(d_{Cu}-d_s)}{2T}\right).$$

This is the expression used to compute all thermal expansion coefficients for our cell.

It may seem appropriate to also take the cell effect into account when making

magnetostriction calculations, however this is unnecessary. Although the size of a sample may change dramatically with changes in magnetic field, the size of OFHC copper hardly varies because copper has no intrinsic magnetism. In fact the cell effect due to magnetic field is two orders of magnitude smaller than data from the material we are measuring. This leaves our definition of linear and volumetric magnetostriction unaltered:

$$m_L = \frac{-1}{d}\frac{2d}{2H};$$

$$m_V = m_a + m_b + m_c.$$

Our Sample

After correcting our thermal expansion data for the cell effect, we were able to calculate the linear thermal expansion and magnetostriction along the c-axis of our sample, $Ce_{.5}La_{.5}RhIn_5$. This compound is a derivative of $CeRhIn_5$, but it is doped with lanthanum so that every other cerium atom is replaced with lanthanum as depicted in Figure 6.

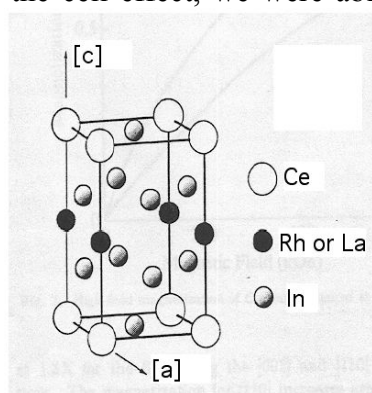

Figure 6: *$CeRhIn_5$ or $Ce_{.5}La_{.5}RhIn_5$*[1]

Cerium is magnetic, making $CeRhIn_5$ paramagnetic at room temperatures and antiferromagnetic below 3.8K. Lanthanum and cerium have very similar chemical properties and atomic weights, therefore doping $CeRhIn_5$ with lanthanum does not change the lattice structure. However, lanthanum is not magnetic, and because of this $Ce_{.5}La_{.5}RhIn_5$ has a lower magnetism than $CeRhIn_5$. The two compounds should still behave similarly, but the effect of the decreased magnetism should also be apparent when comparing different properties of the material. Thermodynamic properties of $CeRhIn_5$, including thermal expansion, have been measured and we expect our results to mimic the published material, but with modified features because of the lanthanum doping. Thermal expansion data for $CeRhIn_5$ has been published by T. Takeuchi et al.[1] and is shown in Figure 7. The important features occur at 3.8K, 25K, and 75K. At 3.8K there is a large peak along the c-axis and slightly smaller peak at the same temperature along the a/b-axes. This feature aligns exactly with a feature in the specific heat and has been identified as a magnetic transition called the Neél Temperature; which signifies a magnetic phase transition between paramagnetism and antiferromagnetism. At 25K there is a strong

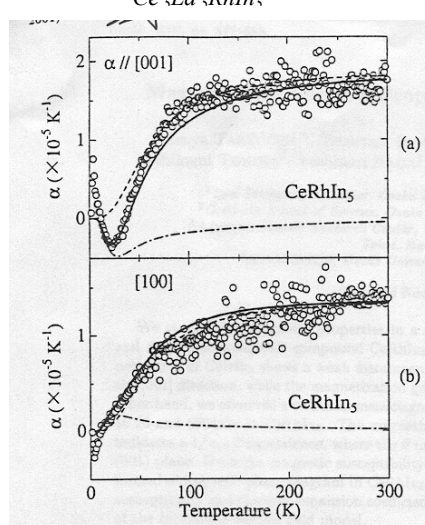

Figure 7: *Linear thermal expansion of $CeRhIn_5$. (a): c-axis and (b): a/b-axes*[1]

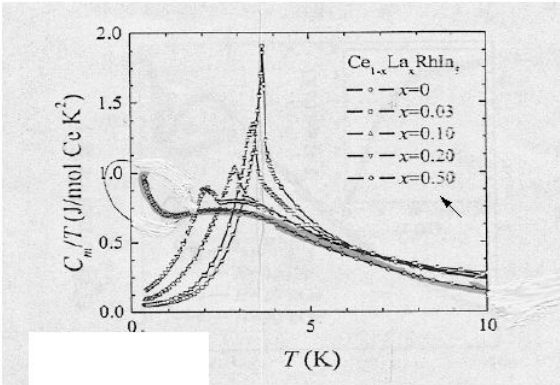

Figure 8: *Suppression of the Neél Temperature with La doping*[2]

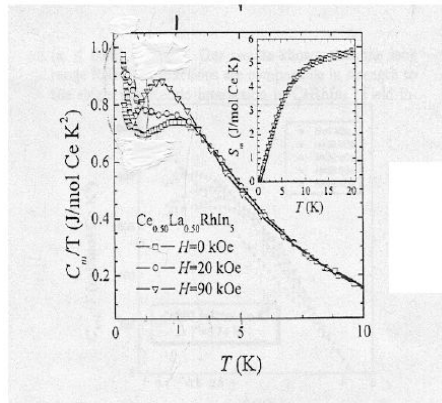

Figure 9: *Transmutation of the Neél Temperature with magnetic field.*[2]

minimum along the c-axis (although no apparent feature along the a/b-axes). The theoretical explanation for this feature involves lifting the six-fold degeneracy in the 4-f levels that is predicted by the crystalline electric field model. Around 75K the two axes mimic each other in a gently sloping increase in α typical of metals. Because of the similarities between $CeRhIn_5$ and $Ce_{.5}La_{.5}RhIn_5$ we expect to see these same features, or very similar features, displaced by the addition of lanthanum.

B.E. Light and A.L Cornelius[2] published heat capacity data for various samples of $CeLaRhIn_5$ ranging from 0-50% lanthanum (Figure 8). It is apparent that as the lanthanum doping increases the Neél temperature shifts to lower temperature and is progressively suppressed. Because doping weakens the magnetic interactions in the material and the Neél temperature marks the transition between two different magnetic phases, this result is not surprising. It is interesting, however, that at a 50% lanthanum doping the Neél Temperature disappears, replaced by a slight hump at 2.5K, and the curve experiences a drastic upturn at low temperatures. The curve's upturn results from a quantum critical point that occurs at 40% lanthanum. At 50% lanthanum the sample is now behaving as a non-Fermi-liquid. The hump, however, cannot be explained by this phase transition and it is proposed that it is due to a certain amount of short range magnetic ordering in the material. To confirm the behavior of $Ce_{1-x}La_xRhIn_5$ around the quantum critical point we measured both a sample that is doped 40% and 50% with lanthanum.

Light and Cornelius went on to measure the heat capacity of 50% lanthanum samples in magnetic fields of various strengths because of the appearance of non-Fermi-liquid behavior at that concentration (Figure 9). Their results show that as the field is increased, the hump grows; which is consistent with the proposal of short range ordering. The upturn due to the non-Fermi-liquid phase translates to higher temperatures with increased field, eventually merging with the hump. We expected to see similar behavior in the magnetostriction of our sample.

A.D. Christianson and A.H. Lacerda[3] measured the resistivity and magnetoresistance of $CeRhIn_5$ and $LaRhIn_5$ along both the c-axis as well as the a/b-axes. The purpose of measuring both these materials is to be able to distinguish the features due to magnetism from the features due to lattice effects and electronic interactions. Their results show the same anisotropy seen in Takeuchi's heat capacity measurements, it is expected that we also witness this directional-dependence in thermal expansion data.

However, resistivity data is not as useful to us as heat capacity because heat capacity, thermal expansion, and magnetostriction are all bulk properties of a material whereas resistivity is a property involving transport—a specific path through the material.

Experiment

Throughout the experiment we used both 20-Tesla and 17-Tesla magnet systems, both with variable temperature insert (VTI) cryostats. Our dilatometer was kept in a vacuum-tight cylindrical brass chamber with a conical seal using high-vacuum grease and Teflon tape (Figure 10). The cryostat is made up of coaxial cylindrical chambers; the outer chamber is filled with liquid nitrogen that is separated from room temperature by a thin layer of vacuum. Another vacuum layer separates the liquid nitrogen from the inner layer; which contains liquid He_4 at 4.2K (and very well isolated from the ambient temperature outside the cryostat). The probe sits inside the VTI which is sealed from the liquid helium except for a small valve, which allows the user to control the amount of He_4 in the VTI. If enough He_4 is allowed in the VTI for the probe to be sitting in a pool of liquid He_4 the minimum temperature the sample would be able to reach would be exactly 4.2K. By pumping the He_4 and decreasing the pressure in the VTI it is possible to bring the temperature down to 1.2K (see the He_4 phase diagram, Figure 11). The temperature is then translated to the sample from the top of the conical seal, through the metal and to the sample space, and also (to a lesser extent) through the sides of the brass chamber and the small amount of gas that is left in the vacuum area. In fact, if the temperature of the sample is observed to cool very quickly it means that more gas than desirable has seeped into the chamber and it is probable that a leak has developed at the seal.

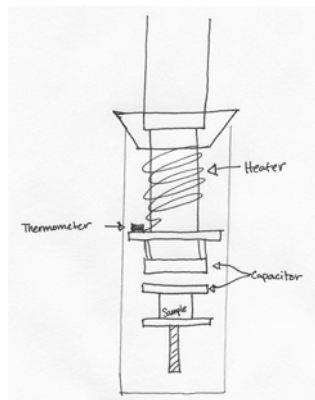

Figure 10: *Dilatometer and probe.*

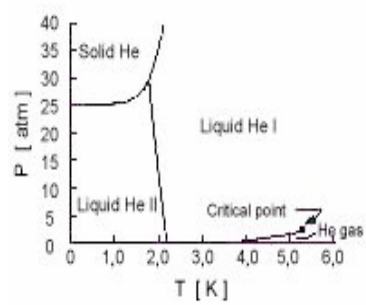

Figure 11: *He_4 phase diagram.*

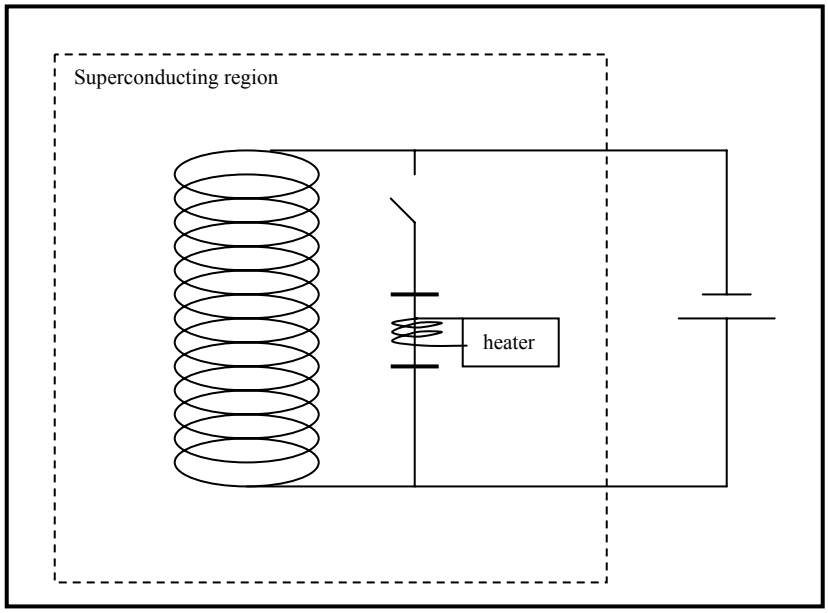

Figure 12: *Electromagnet circuit model.*

The electromagnets are superconducting coils of Nb_3Sn intertwined with copper. The copper acts as a low-resistance alternate route for current at room temperature. In the event of a quench—where the magnet unexpectedly becomes non-superconducting and suddenly has a lot of energy to transfer—Nb_3Sn becomes non-superconducting and has a substantial resistance, so the current will instead travel through the copper. The copper wire creates less heat and conducts more efficiently, and will hopefully alleviate some of the stress on the system if a quench does indeed occur. The coils are situated within the liquid helium and kept at or below 4.2K. If the temperature of the coils ever rises above the critical temperature of Nb_3Sn (~10K) they will become non-superconducting and the magnet will quench.

The circuit diagram in Figure 12 shows roughly how a superconducting magnet operates. Current from the power source enters the coils and will circulate in the superconducting region as long as the heater is off. After the current is introduced into the superconducting circuit the source can be disconnected. Increasing the field from this point is as straightforward as increasing the current, but it is important to remember that the current must be increased slowly to avoid a large amount of induced flux through the coils. It is more difficult to reduce the field of the magnet. For example, if you were to turn on the heater without supplying any current from the source, the current in the coils would dissipate quickly through the heated portion of wire (this portion of the wire is carefully contained by balancing thermal conductivity and heat capacity of the material of the wire) and the induced flux could breach the current limitation for superconducting Nb_3Sn and quench the magnet. Instead, you should supply a current from the source equal to that within the coils. This makes it possible to dissipate current through the heater without inducing any flux. From this point, the current can be slowly decremented from the source to reduce the magnetic field. As long as the current is reduced slowly there is no risk of quenching. Once the desired field is reached, the source and the heater can again be cut off, leaving the remaining current to circulate indefinitely in the

superconducting region.

To take measurements we are using a Lakeshore DRC-91CA temperature controller, an Andeen Hagerling 2500A 1kHz capacitance bridge, and a Oxford PS 180 current source. Two ways in which to take measurements are continuously or with a temperature series. They are both controlled externally with LabView (a data acquisition program). A temperature series is a user specified series of set points. This method requires a program that will reset the set point when called on to do so to the next requested value. The continuous mode simply communicates with the computer as fast as requested (or to the capability level of the instruments). The temperature controller is wired to a thermometer inside our dilatometer. Because temperature is just a function of resistance specific to a material, these two quantities are interchangeable and the resistance of a material can be used to measure temperature. An effective thermometer functions as a metal at high temperatures and a semiconductor at low temperatures. At low temperatures a plot of resistance versus temperature for a semiconductor has a very steep slope, allowing a slight change in resistance to correspond to a significant change in temperature. Likewise, a metal at higher temperatures has a considerable slope and its resistance translates fairly accurately into temperature.

The Andeen Hagerling capacitance bridge measures the capacitance between the plates of the dilatometer using a Wheatstone-like bridge circuit. Because of the shape of the Wheatstone circuit (Figure 13), the unknown capacitance (C_x) can be calculated from the relationship,

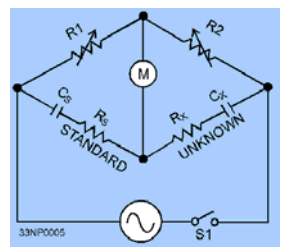

Figure 13: *Wheatstone Capacitance Bridge Circuit.*

$$\frac{R_1}{R_2} = \frac{C_x}{C_s}.$$

Using this expression, the bridge can accurately determine an unknown capacitance (such as the capacitance in our dilatometer).

Finally, because the user controls the flow of current into the coils of the magnet, the blah can easily compute the corresponding magnetic field using the following physical law:

$$\mathbf{B} = n_0 N \mathbf{I},$$

where **B** is the magnetic field in the direction of the current through the coils, μ_0 is the permeability of free space ($4\pi \times 10^{-7}$), N is the number of coils per unit length, and **I** is the current through the coils.

The magnet source, capacitance bridge, and temperature controller must all communicate with the computer program to record various capacitances and the temperatures or magnetic fields that they are associated with. One potential problem that can provide inaccurate data is an inconsistency between the temperature at the thermometer and the temperature of the sample and the capacitor plates. In hopes to prevent this from occurring, the dilatometer is constructed to be an excellent thermal conductor and can transfer heat quickly and uniformly throughout the cell. If, however, the cell is heated or cooled too quickly this disparity could still occur, and the collected

data will be erroneous. Care should be taken to change the temperature of the cell slowly when using the continuous method of measurement to ensure accurate data.

An alternative to this approach is to take data with a temperature series. The temperature series function has a built in system that tests for fluctuations before taking a measurement. It will first acquire a set point from a series of temperatures created by the user, then use an equipment specific gain curve defined as a polynomial: $a^2T+bT+c$, to set three parameters calculated from the gain curve and the given set point: percentage, integral, and derivative (PID). These parameters are used to deduce the most efficient heating scheme to reach the requested set point. Once the temperature is within two percent of the desired set point, the program will begin to check for stabilization. It determines temperature stability by checking that sixty independent measurements taken every three seconds are within 20mK of each other. Once temperature stability is established, the program checks the stability of the capacitance value by calculating the derivative of capacitance with respect to time and will only take a measurement when this quantity is sufficiently low. As might be expected, using this process takes a long time. The highest efficiency is dependent on the accuracy of the gain curve, and even with the most accurate curve possible one measurement takes a minimum of three minutes. This accuracy is hard to achieve, it could take days to find the right gain curve. The measurements we took in the 15 Tesla system took about 3 minutes per data point at low temperatures and sometimes over 20 minutes at higher temperatures. A series of data could take between 20 and 24 hours of measuring.

Our Measurements

Most of our thermal expansion measurements were taken warming up (rather than starting at room temperature and cooling down) with a temperature series because of the heightened accuracy of the procedure. We mounted the sample so that we would be measuring along the c-axis, polishing the surfaces so that the capacitance plates would indeed lie parallel to each other. The data we collected was very smooth—a good sign because any variation is magnified when taking the derivative to calculate thermal expansion or magnetostriction. From the collected data we were able to calculate the linear thermal expansion coefficient and the coefficient of magnetostriction using formulas stated above and two data analysis programs: Igor and Origin. I mostly used Igor and Victor used Origin as a result of office computer space—Origin is limited to PC's where Igor is compatible with both. Both of us experimented with different ways of analyzing the data that would preserve the real shape of the curve while minimizing noise and unwanted fluctuations. For example, it turned out to be more accurate to take the derivative before interpolating to the number of necessary data points rather than interpolating points that might alter the derivative of the data. I also made a point to use smoothing curves as late as possible in the analysis to avoid smoothing out important details, and used Igor's most accurate technique for differentiating and fitting smoothing curves: cubic spline. Cubic spline fits a cubic polynomial to three data points and interpolates and differentiates along that polynomial. The more common alternative to this method is to interpolate along a linear curve between points and look only at directly

neighboring points to perform a derivative.

Magnetostriction

We measured the magnetostriction of a 1.51mm sample of $Ce_{.5}La_{.5}RhIn_5$ at three different temperatures: 1.65K, 2.99K, and 8.95K (these were the values where the temperature remained stable). Figure 14 shows a plot of the coefficient of magnetostriction versus applied magnetic field for these values. Notice that each set of data very closely follow the same linear relationship. This is convincing evidence that our sample is exhibiting itinerant paramagnetism. We can show this by starting with the definition:

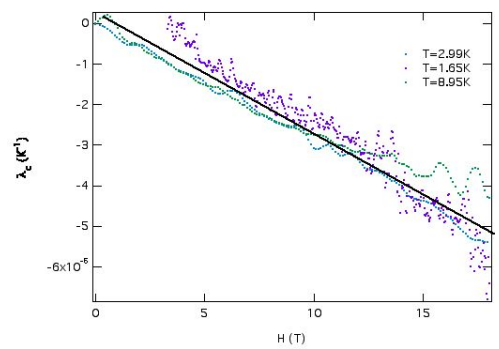

Figure 14: *Linear magnetostriction coefficient versus magnetic field.*

$$B = H + 4\pi M,$$

where B is the intrinsic magnetic field of the material, H is the applied field, and M is the magnetization. At these temperatures we expect our material to be paramagnetic because of the 50% lanthanum doping suppressing the Neél temperature to zero as seen in Figure 8. Therefore we can use an expression for the magnetism of paramagnetic materials:

$$M = \chi H,$$

where χ is the magnetic susceptibility. Substituting into the equation above:

$$B = H + 4\pi\chi H = (1 + 4\pi\chi)H.$$

The Curie-Weiss Law states:

$$\chi = \frac{C}{T - T_c};$$

and is the general law for localized paramagnetism, where C is the Curie constant, and T_c is the Curie temperature. In our case, this law simplifies to:

$$\chi = \frac{C}{T}.$$

Substituting this quantity from the equation for B above,

$$B = \left(1 + 4\pi \frac{C}{T}\right)H.$$

Now we must engage our definition of magnetostriction:

$$\mu_V V = \left(\frac{\partial V}{\partial H}\right)_{T,P},$$

and some Maxwell relations:

$$\left(\frac{\partial V}{\partial H}\right)_{T,P} = \frac{1}{4\pi}\left(\frac{-\partial B}{\partial P}\right)_{H,T} = \mu_V V.$$

Finally, if we differentiate the above equation for magnetic field (B) with respect to pressure,

$$\left(\frac{-\partial B}{\partial P}\right)_{H,T} = \frac{-\partial}{\partial P}\left(\frac{1}{4\pi} + \frac{C}{T}\right)_{H,T} H.$$

Noting that the only variable that changes with pressure is the Curie constant we now have:

$$\mu_V V = \frac{-H}{T}\left(\frac{\partial C}{\partial P}\right)_{H,T}.$$

In this instance $\partial C/\partial P$ is constant because we are not varying the pressure of the system, and it is now clear that the linear behavior of Figure x shows that our sample is indeed paramagnetic at these temperatures. It is also apparent from Figure x and the above expression that the magnetostriction must be temperature independent; otherwise the slopes of the magnetostriction coefficients would be change with various values of temperature. This temperature independent linearity could be caused by itinerant (or metallic) paramagnetism; which is magnetism caused by valence electrons rather than electrons bound by atoms. The valence electrons do not directly affect the structure of the lattice and therefore changes in their magnetic moments due to varying temperatures would not change the magnetostriction of the material.

<u>Thermal Expansion</u>

We initially measured the thermal expansion of $Ce_{.5}La_{.5}RhIn_5$ using the 1.51mm sample, and found that a sample of such small dimensions produces unpleasant data, as shown in Figure 15. A sample of this size has a thermal expansion comparable to noise and unavoidable fluctuations that are inevitable in measurements. The data in Figure 15 has been smoothed and interpolated, and although this improves its aesthetic appearance this analysis can be deceiving, as the oscillations look too regular to be noise. However, calculations performed without any smoothing showed that these oscillations are undoubtedly noise. Another feature of this data that makes it unreliable is the fact that it cannot be easily extrapolated to zero. This breaks fundamental laws of thermodynamics and is not believable.

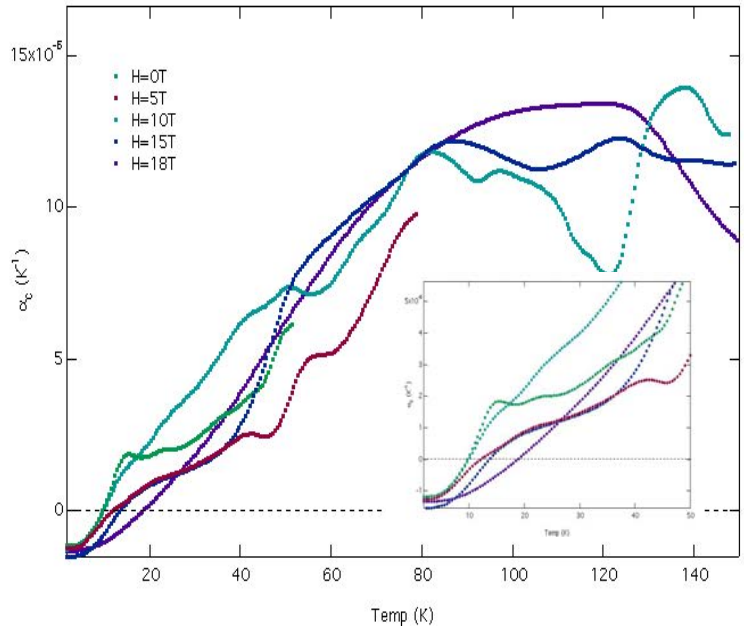

Figure 15: *Linear thermal expansion coefficient of $Ce_{.5}La_{.5}RhIn_5$ versus temperature.*

Luckily we were able to acquire another sample with much larger dimensions: 3.06mm along the c-axis. There is one difference, however, in that the 3.06mm sample is doped with 40% lanthanum where our previous sample is doped with 50% lanthanum. This difference is not too significant; $CeRhIn_5$ doped with 40% La is still within the range of the quantum phase transition, and will still supply satisfactory data for studying this transition. Our results are shown for fields of zero and 18T in Figure 16, and the improvement over the smaller sample is phenomenal. First of all, the data shift regularly with applied magnetic field, where the above data from the 1.51mm

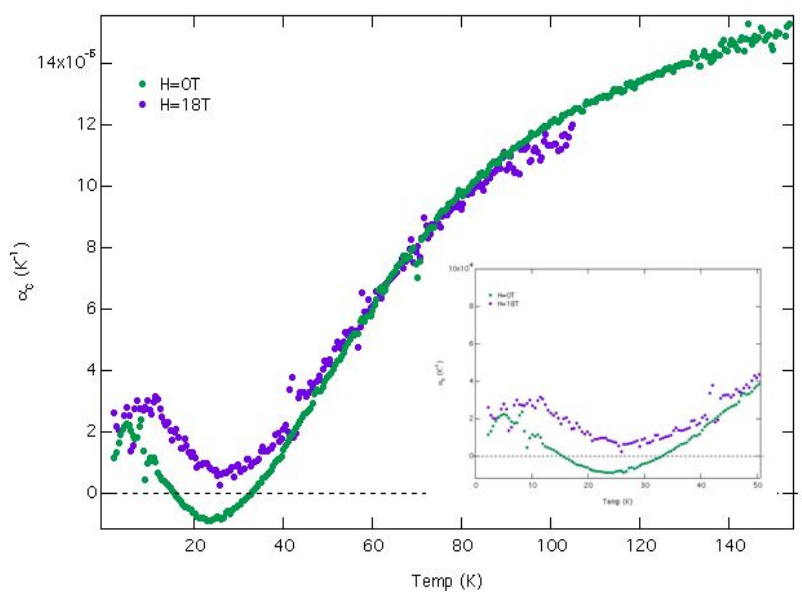

Figure 16: *Linear thermal expansion coefficient of $Ce_{.6}La_{.4}RhIn_5$ versus temperature.*

sample cross each other often and do not seem to have much of a tendency to arrange with field. Furthermore, the data in Figure 16 is not smoothed (interpolation is necessary to perform the calculation) it follows a very distinct path and smoothing would only suppress the real data. An important feature to note is the minimum at 20K. A similar feature is seen in the linear thermal expansion along the c-axis of $CeRhIn_5$ as measured by Takeuchi et al. (Figure 7), which is attributed to crystalline electric field contributions. This consistency with published data gives us confidence in our own. Other reassuring attributes of our data are that the behavior of the coefficient of thermal expansion above 100K very closely mimics that of a normal metal, and, most importantly, the data appears to extrapolate nicely to zero.

An interesting addition to data published by Takeuchi et al. is that there is a progression of the feature at 20K from a negative thermal expansion (shrinking material) to a positive thermal expansion (expanding material) induced solely by applying field. Another important characteristic of these data is the maximum that occurs around 4.6K, which could correspond to the hump at 2.5K seen in heat capacity data for a 50% La sample in the paper by Light and Cornelius (see Figure 8 above). In their paper, this hump was attributed to short range ordering, and tends to become more substantial with field. It is hard to tell whether this is the trend in our data, but it is not unlikely. This maximum is more easily seen in data taken at 10T from 1.7K to 6K shown in Figure 17 with a very simple polynomial extrapolation that hits 0K perfectly. (The data is plotted as $\partial C/\partial T$, which ultimately has the same shape as α_c because the cell effect makes no significant contribution at these temperatures.) Another possible explanation for this apparent maximum is a reappearance of the Neél temperature. Because this sample is doped with 40% La it is possible that it is still in a region below the quantum critical point, where a transition into an antiferromagnetic state may occur at very low temperatures. It is possible, however, that the temperature at which this maximum is observed is too high to be a possible magnetic phase transition.

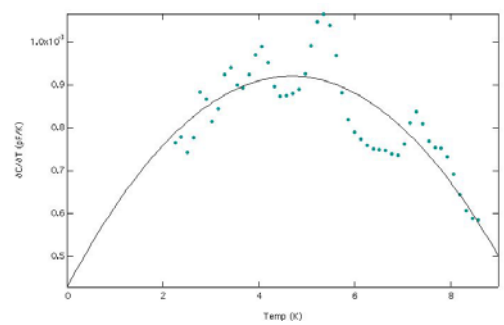

Figure 17: *$\partial C/\partial T$ versus temperature for $Ce_{.6}La_{.4}RhIn_5$ at 10T*

Conclusion

It is clear that more data is needed for definite results of this experiment. Luckily, this project is still in progress and further data is being collected daily, including magnetostriction data for the 3.06mm sample, thermal expansion at lower temperatures, another measurement of the cell effect in order to improve calculations, and—most importantly—a rotation of the sample to analyze the a/b-axes and calculate the volumetric thermal expansion and magnetostriction of $Ce_{.6}La_{.4}RhIn_5$ and possibly $Ce_{.5}La_{.5}RhIn_5$.

Acknowledgements

I had an unlimited amount of support this summer from everybody at NHMFL. It was a great learning experience, and I couldn't have asked to be in a better environment. I'd especially like to than Alex Lacerda and Victor Correa for their innumerable explanations and everyday guidance.

References

[1]Tetsuya Takeuchi, Tetsutaro Inoue,Kiyohiro Sugiyama, Dai Aoki, Yoshihumi Tokiwa, Yoshinori Haga, Koichi Kindo, and Yoshichika Onuki. Journal of the Physical Society of Japan. Vol. 70, No. 3 (2001).

[2]B.E. Light, A.L. Cornelius, P.G. Pagliuso, and J.L. Sarrao. Cond-mat/0307394.

[3]A.D. Christianson, A.H. Lacerda, M.F. Hundley, P.G. Pagliuso, and J.L. Sarrao. Phys. Rev. B **66**, 054410 (2002).